ISSN 1 746-7233, England, UK
World Journal of Modelling and Simulation
Vol. 5 (2009) No. 4, pp. 315-320

Elasto-hydrodynamic lubrication analysis of full 360° journal bearing using CFD and FSI techniques

B. S. Shenoy*, R. S. Pai, D. S. Rao, R. Pai

Department of Mechanical and Manufacturing Engineering, Manipal Institute of Technology, Manipal, Karnataka 576104, India

(*Received March 20 2009, Accepted July 27 2009*)

Abstract. Conventional method of performing an EHL analysis on a bearing involves development of complex codes and simplification of actual physical model. This paper presents a methodology to model and simulate the Overall Elasto-Hydrodynamic Lubrication of a full journal bearing using the sequential application of Computational Fluid Dynamics (CFD) and Computational Structural Dynamics (CSD). Here, the coupled field analysis uses the capabilities of commercially available Finite Element Software ANSYS/FLOTRAN incorporating the technique of Fluid Structure Interaction (FSI). The pressure field for a full journal bearing operating under laminar flow regime with various L/D ratios is obtained by CFD. Stress distribution and deformation in the bearing liner due to resulting pressure force is evaluated using FEM, satisfying the boundary conditions. The stress distribution indicates the critical points in the bearing structure. The results show reasonable agreement in general.

Keywords: journal bearings, eccentricity ratio, L/D ratio, CFD, FSI, EHL

1 Introduction

Journal bearings have the longest history of scientific study of any class of fluid film bearings. In a fluid film bearing, the pressure in the oil film satisfies the Reynolds equation which intern is a function of film thickness. Structural distortion of the housing and the development of hydrodynamic pressure in a full journal bearing are strongly coupled thus require a combined solution. Traditional method of lubrication analysis proposed by researchers like Reddi[8], Wada[9, 10], Huebner[3] and Allaire[1] involves the development of complicated numerical calculation programs as well as the simplification of the actual physical model. However, other researchers as Tucker[12], Chen[5] and Brajdic-Mitidieri[4] applied the CFD codes to make the analysis effective when complex flow geometries are involved or when solutions that are more detailed are needed. Hirano[7, 11] carried out a study to simulate the pressure field and calculate the performance characteristics of bearings and seals. Based on the multi-physics approach, Praveen[2] recently analyzed EHL in partial arc bearings.

This paper presents a methodology to model and simulate the Overall Elasto-Hydrodynamic Lubrication of a full journal bearing using the sequential application of Computational Fluid Dynamics (CFD) and Computational Structural Dynamics (CSD).

2 Theory

2.1 Fluid structure interaction

* Corresponding author. Tel.: +918202925462, fax: +918202571071; *E-mail address*: satishshenoyb@yahoo.com.

In fluid-structure interaction (technically fluid-solid), fluid flow exerts pressure on a solid structure causing it to deform such that it alters the initial fluid flow. Fluid Structure Interaction occurs in physics simulation wherever the problem involves the flow of fluid causing the deformation of a solid structure. The deformation of a solid structure; in turn, changes the boundary condition of the fluid problem. A general FSI solver algorithm consists of the time stagger and the field loop. Blending all of the separate physics fields into one multi-physics analysis is to be performed automatically by the solver. Physics fields "interact" with one another through surface or volumetric interfaces, and field coupling is achieved by mapping loads from one field mesh to another. Moreover, the convergence criterions are to be monitored at the interfaces where the loads are transferred.

The interaction of the fluid and the structure at the mesh interface causes the pressure to exert a force applied to the structure and the structural motions produce an effective "fluid load". The governing finite element equations are given as:

$$[\boldsymbol{M}_s]\{\ddot{U}\} + [K_s]\{U\} = [\boldsymbol{F}_s] + [\boldsymbol{R}]\{P\}\,. \tag{1}$$

$$\begin{bmatrix} \boldsymbol{M}_s & 0 \\ \rho \boldsymbol{R}^T & \boldsymbol{M}_f \end{bmatrix} \begin{Bmatrix} \ddot{U} \\ \ddot{P} \end{Bmatrix} + \begin{bmatrix} K_s & -\boldsymbol{R} \\ 0 & K_f \end{bmatrix} \begin{Bmatrix} U \\ P \end{Bmatrix} = \begin{Bmatrix} \boldsymbol{F}_s \\ \boldsymbol{F}_f \end{Bmatrix}. \tag{2}$$

Where, $[\boldsymbol{M}_S]$ is the structural mass matrix; $[\boldsymbol{M}_f]$ is the fluid mass matrix; $[\boldsymbol{F}_s]$ and $[\boldsymbol{F}_f]$ is the structural and fluid force matrix; $[\boldsymbol{R}]$ is a coupling matrix that represents the effective surface area associated with each node in fluid structure interface.

The coupling matrix also takes into account the direction of the normal vector defined for each pair of coincident fluid and structural element faces comprises the interface surface. The positive direction of the normal vector, as the ANSYS program uses it, is defined to be outward from the fluid mesh and is towards the structure. Both the structural and fluid quantities that are produced at the fluid structure interface are functions of the unknown degree of freedom. Placing these unknown load quantities on the left hand side of the equations. The above equation implies that nodes on a fluid structure interface have both displacement and pressure degree of freedom.

2.2 Mapping

In order to transfer loads across a dissimilar mesh interface, the nodes of one mesh must be mapped to the local coordinates of an element in the other mesh. The Multi Field Solver solution algorithm must perform two mappings for every surface to surface and volume to volume interface. In the fluid film analysis, fluid nodes must be mapped to the solid elements to transfer displacements. Likewise, solid nodes must be mapped to the fluid elements to transfer stresses.

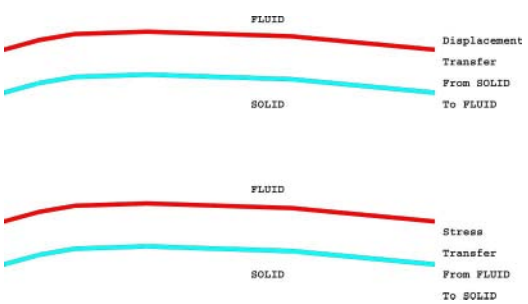

Fig. 1. Fluid Solid Interaction load transfer

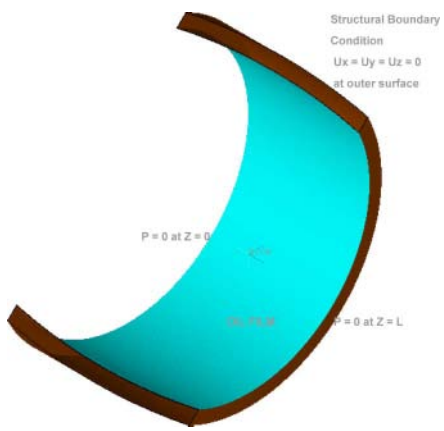

Fig. 2. Boundary conditions

2.3 Mesh updating

Many a time coupled-field analysis involving a fluid domain and a structural domain yields significant structural deflections. In this case, to obtain an overall converged coupled-field solution it is often necessary to update the finite element mesh in the non-structural region to coincide with the structural deflection and recursively cycle between the field solution and structural solution. Mesh Morphing Technique is used to move nodes and elements of the "field" mesh to coincide with the deformed structural mesh.

Software involved in the analysis of FSI should provide a strong coupling between CFD and CSD. During every computational step, the fluid flow field and the structure evolve as a coupled system. ANSYS program can perform multi-physics analyses with a single ANSYS database. A single set of nodes and elements will exist for the entire model. Representation of these elements changes from one physics analysis to another, based on the use of the physics environment concept. Across multi-physics environments, element types must maintain a consistent base geometry.

3 Methodology

The procedure for doing a FSI analysis of a full journal bearing consists of four main steps:

- Setup the fluid and solid analyses;
- Flag fluid-solid interfaces;
- Specify the fluid-solid interaction solution options;
- Obtain and Post process the results.

3.1 Setup the fluid and solid analysis

To perform a fluid-solid interaction analysis for elasto-hydrodynamic Lubrication, first create the oil film model and the finite element mesh for this region. Apply the appropriate boundary conditions, as shown in Fig. 2, material properties for the fluid analysis, and select the appropriate solution options. Create the solid model of the bearing housing and the finite element mesh for this region. Apply the appropriate boundary conditions and material properties for the structural analysis, and select the appropriate solution options.

3.2 Flag fluid-solid interfaces

The next step is to flag film-bearing interface where load transfer takes place with a FSI number. Apply the field-surface interface flag twice: once for the fluid side of the interface and once for the solid side of the interface. Load transfer occurs between film and bearing interface with the same interface number.

3.3 Specify the FSI solution options

This section discusses the options that are required to specify the film-bearing interaction solution.

- Specify basic analysis options like the solution order, the interpolation method and the method for load transfer across the interface;
- Maximum number of stagger iterations (depends on convergence criterion);
- Convergence values (0.5e-2);
- Specify output frequency (100);
- Specify relaxation values (0.5).

3.4 Obtain and post process the results

The analysis is performed in ANSYS/FLOTRAN and the results are obtained. To post process FSI analysis, the database must be resumed. A Standard ANSYS macro is written according to the flow chart shown in Fig. 3. You can review results using standard ANSYS postprocessor commands. Simultaneous post processing of the fluid and solid results files is not supported. Read in the fluid or the solid result file one at a time and post process the results.

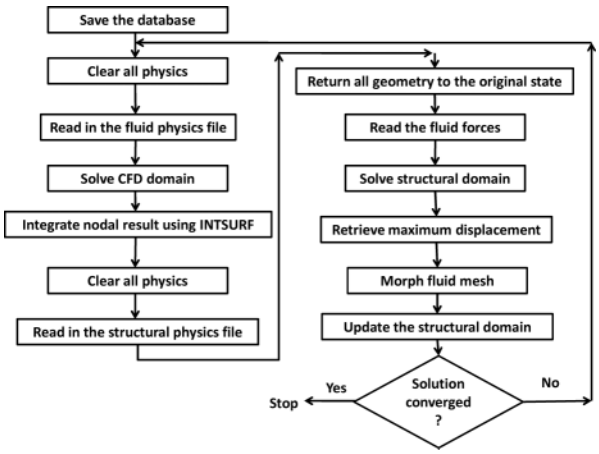

Fig. 3. Flow chart for performing a Fluid Structural Interaction simulation

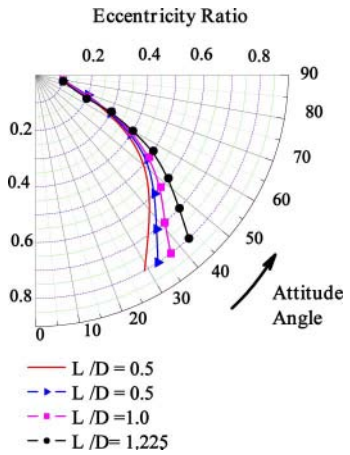

Fig. 4. Comparison of Attitude angle from the present analysis with Ref [6], for bearing with L/D $= 0.5$

4 Solution procedure

Standard ANSYS macro is developed to simulate the EHL of a full journal bearing (360°). Modeling is done as per the details given in Tab. 1. Cavitation is modeled by setting all calculated negative pressure and their gradients equal to zero throughout the iteration. The iteration is repeated until the pressure satisfies the convergence criterion. Static performance characteristics such as load carrying capacity and shaft attitude angle are evaluated by integrating the hydrodynamic pressure over the bearing surface.

Table 1. Details of full journal bearing

Journal radius (R_j)	0.05 m
Radial clearance (C)	50 μm
Bearing pad thickness (t)	0.005 m
Length to diameter ratio (L/D)	0.5, 1.0 and 1.225
Eccentricity ratio (ε)	0.2 to 0.8
Youngs modulus (E)	200 Gpa
Poissons ratio (μ)	0.3
Operating speed (N)	2000 rpm
Lubricant Density (ρ)	835 kg/m^3
Lubricant Viscosity (μ)	0.0125 $N - s/m^2$

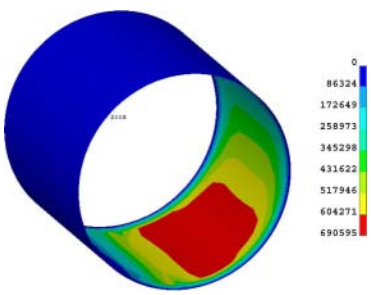

Fig. 5. Pressure contour for a bearing with L/D $= 1.0$, $\varepsilon = 0.6$

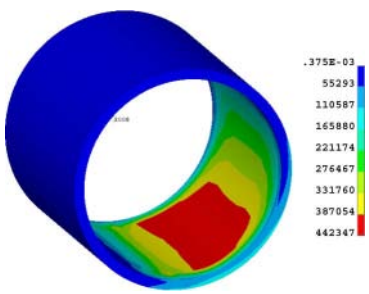

Fig. 6. Stress Contour for a bearing with L/D $= 1.0$, $\varepsilon = 0.6$

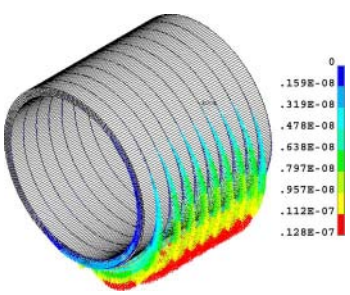

Fig. 7. Deformation vector plot for a bearing with L/D $= 1.0$, $\varepsilon = 0.6$

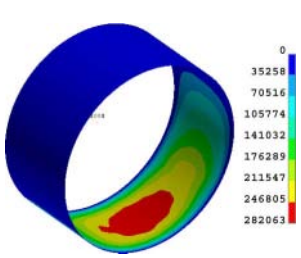

Fig. 8. Pressure contour for a bearing with L/D $= 0.5$, $\varepsilon = 0.2$

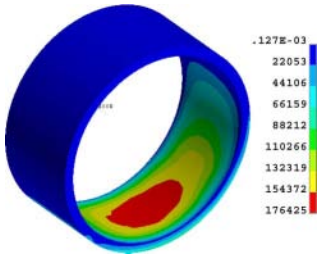

Fig. 9. Stress Contour for a bearing with L/D $= 0.5$, $\varepsilon = 0.2$

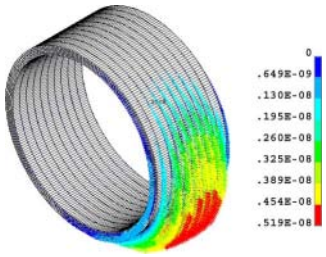

Fig. 10. Deformation vector plot for a bearing with L/D $= 0.5$, $\varepsilon = 0.2$

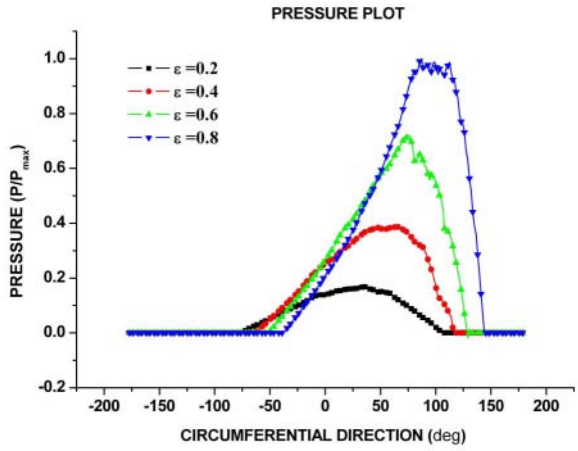

Fig. 11. Pressure plot (mid-plane) in the bearing for L/D $= 1.0$

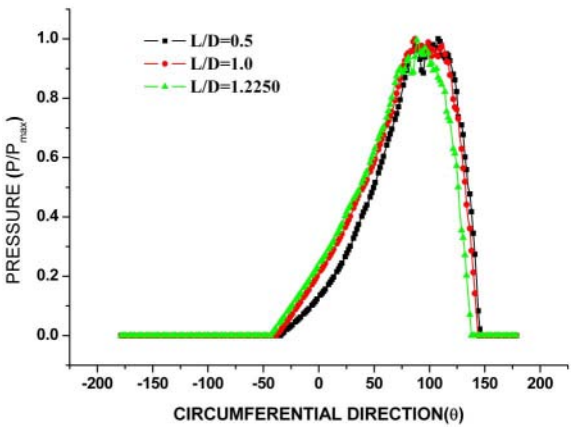

Fig. 12. Pressure (mid-plane) in the bearing for $\varepsilon = 0.6$

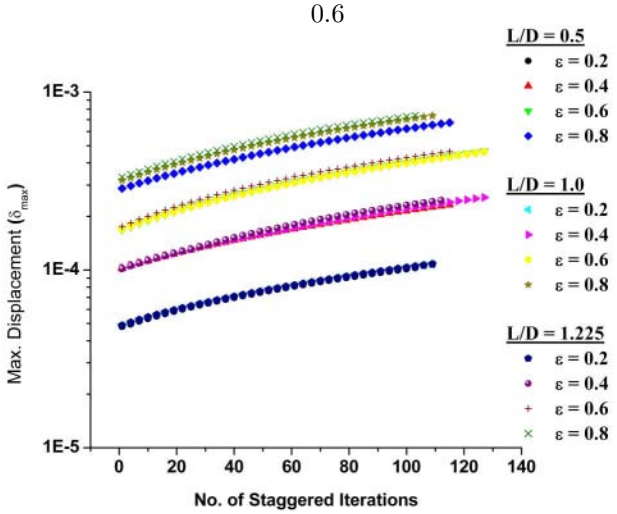

Fig. 13. Plot of maximum displacement Vs the number of staggered iterations for various L/D ratios and ε

5 Results and discussions

To validate the present methodology, shaft attitude angle obtained from the present analysis for different values of L/D and ε, as shown in Fig. 4, is compared with the illustrations of Dubios[6].

Fig. 5 shows the hydrodynamic pressure developed in the oil film for L/D $= 1.0$ and $\varepsilon = 0.6$. Moreover, Fig. 6 and Fig. 7 depicts the stress distribution and the displacement vectors in the bearing housing for L/D $= 1.0$ and $\varepsilon = 0.6$, respectively. Fig. 8 $\sim$ Fig. 10 illustrate the simulation results for a study with $\varepsilon = 0.2$ and L/D $= 0.5$. From Fig. 5 $\sim$ Fig. 7 and Fig. 8 $\sim$ Fig. 10, it is observed that the extent of hydrodynamic pressure, stress and the housing deformation for a bearing with L/D $= 1.0$ and $\varepsilon = 0.6$ is higher than the one with L/D $= 0.5$ and $\varepsilon = 0.2$.

Fig. 11 shows variation of the pressure (mid-plane) developed in the circumferential direction for bearing with L/D $= 1.0$ for different values of ε. Similarly, Fig. 12 illustrates the effect of various L/D on the pressure distribution for $\varepsilon = 0.6$. From Fig. 11 and Fig. 12 it is clear that ε has greater influence on the pressure than L/D ratios. Fig. 13 compares the maximum deformation of the bearing structure with various L/D and ε. From Fig. 13 it is observed that an increase in ε predominantly increases $\delta_{\max}$.

6 Conclusions

The overall EHL analysis of full journal bearing (360°) has been conducted using the sequential application of Computational Fluid Dynamics (CFD) and Computational Structural Dynamics (CSD). General FSI codes makes the analysis effective where complex flow geometries are involved or when more detailed solutions are needed. The simulation results of Elasto-hydrodynamic lubrication have a good agreement with that of the standard lubrication solutions. These techniques has been successfully implemented in finding the bearing surface deformation under static load and the approach can be extended in predicting the bearing performance under dynamic loading condition. Eventually FSI analysis will play a very important role in the field of fluid film bearing analysis.

References

[1] P. Allaire, J. Nicholas, E. Gunter. Systems of Finite Elements for finite bearings. *ASME Journal of Lubrication Technology*, 1972, (99): 187–197.

[2] P. Bhat, B. Shenoy, R. Pai. Elasto-hydrodynamic Lubrication Analysis of a Radialy Adjustable Partial Arc Bearing Using Fluid Structure Interaction. **in:** *Proc. of ASME/STLE International Joint Tribology Conference*, San Diego, California, US, 2007, 1–3. IJTC'07, IJTC44479.

[3] J. Booker, K. Huebner. Application of Finite Element Methods to Lubrication: an Engineering Approach. *ASME Journal of Lubrication Technology*, 1972, (94): 313–323.

[4] P. Brajdic-Mitidieri, A. Gosman, et al. CFD Analysis of a Low Friction Pocketed Pad Bearing. *ASME Journal of Tribology*, 2005, **127**(4): 803–812.

[5] P. Chen, E. Hahn. Use of Computational Fluid Dynamics in Hydrodynamic Lubrication. *Proceedings of Institute of Mechanical Engineers: Part J, Journal of Engineering Tribology*, 1998, (6): 427–435.

[6] B. George, W. Fred. Analytical Derivation and Experimental Evaluation of Short Bearing Approximation for Full Journal Bearings. *NACA TN*, 1953, 1199–1230.

[7] Z. Guo, H. Toshio, R. Gordon. Application of CFD Analysis for Rotating Machinery Part1: Hydrodynamic, Hydrostatic Bearings and Squeeze Film Damper. *Journal of Engineering for Gas Turbines and Power*, 2005, **127**(2): 445–451.

[8] M. Reddi. Finite-Element Solution of the Incompressible Lubrication Problem. *ASME Journal of Lubrication Technology*, 1969, **91**(3): 524–533.

[9] W. Sanae, H. Hirotsugu. Application of Finite Element Method to Hydrodynamic Lubrication Problems: Part 2, Finite Width Bearings. *Bulletin of the JSME*, 1971, **14**(77): 1234–1244.

[10] W. Sanae, H. Hirotsugu, M. Masakazu. Finite Element Method to Hydrodynamic Lubrication Problems: Part 1, Infinite Width Bearings. *Bulletin of the JSME*, 1971, **14**(77): 1222–1233.

[11] H. Toshio, Z. Guo, R. Gordon. Application of Computational Fluid Dynamics Analysis for Rotating Machinery-Part II: Labyrinth Seal Analysis. *Journal of Engineering for Gas Turbines and Power*, 2005, **127**(4): 820–826.

[12] P. Tucker, P. Keogh. A Generalized Computational Fluid Dynamics Approach for Journal Bearing Performance Prediction. **in:** *Proceedings Institution of Mechanical Engineers: Part J, Journal of Engineering Tribology*, 3, 1994, 99–108.